

## A NEW VIEW OF THE DWARF SPHEROIDAL SATELLITES OF THE MILKY WAY FROM VLT/FLAMES<sup>1</sup>: WHERE ARE THE VERY METAL POOR STARS?

AMINA HELMI<sup>2</sup>, M.J. IRWIN<sup>3</sup>, E. TOLSTOY<sup>2</sup>, G. BATTAGLIA<sup>2</sup>, V. HILL<sup>4</sup>, P. JABLONKA<sup>5</sup>, K. VENN<sup>6</sup>, M. SHETRONE<sup>7</sup>, B. LETARTE<sup>2</sup>, N. ARIMOTO<sup>8</sup>, T. ABEL<sup>9</sup>, P. FRANCOIS<sup>4,10</sup>, A. KAUFER<sup>10</sup>, F. PRIMAS<sup>11</sup>, K. SADAKANE<sup>12</sup>, T. SZEIFERT<sup>10</sup>

*Draft version November 14, 2006*

### ABSTRACT

As part of the Dwarf galaxies Abundances and Radial-velocities Team (DART) Programme, we have measured the metallicities of a large sample of stars in four nearby dwarf spheroidal galaxies (dSph): Sculptor, Sextans, Fornax and Carina. The low mean metal abundances and the presence of very old stellar populations in these galaxies have supported the view that they are fossils from the early Universe. However, contrary to naive expectations, we find a significant lack of stars with metallicities below  $[\text{Fe}/\text{H}] \sim -3$  dex in all four systems. This suggests that the gas that made up the stars in these systems had been uniformly enriched prior to their formation. Furthermore, the metal-poor tail of the dSph metallicity distribution is significantly different from that of the Galactic halo. These findings show that the progenitors of nearby dSph appear to have been fundamentally different from the building blocks of the Milky Way, even at the earliest epochs.

*Subject headings:* Galaxies: abundances – Galaxies: dwarf – Galaxies: evolution – Local Group – Galaxy: formation – Galaxy: halo – Stars: abundances – Cosmology: early universe

### 1. INTRODUCTION

The relevance of dwarf galaxies in the Local Group is twofold. As nearest neighbour systems, they can be studied in great detail and hence they are excellent cases for understanding star formation and prototypical galaxy evolution over the lifetime of the Universe (Mateo 1998). Furthermore, dwarf galaxies are the simplest systems and have universal relevance as they are potentially the building blocks of larger galaxies.

All the dSph satellites of the Milky Way contain a population of very old stars and have low mean metallicities similar to those found in the Galactic stellar halo (Grebel & Gallagher 2004). Because the metallicity of a galaxy increases in time, the most metal-poor stars must be related to the first stars formed, allowing direct access to the physical processes and properties of the early Universe. For example, if dSph were fossils of the pre-reionization era (Gnedin & Kravtsov 2006), the first stars in them could have been (partly) responsible for the reionization of the Universe and the metal-enrichment of the intergalactic medium (Bromm & Larson 2004).

*Present-day* dSph have been ruled out as the prime contributors to the Galactic halo on the basis of their stellar populations (Unavane, Wyse & Gilmore 1996) and their detailed chemical abundance patterns (Shetrone, Côté & Sargent 2001; Venn et al. 2004; Pritzl, Venn & Irwin 2005). This is not completely unexpected given that the surviving dSph have had a Hubble time to evolve as independent entities under differing conditions. Font et al. (2006) point out that if the dSph had been accreted at early epochs, they could still have been the building blocks of hierarchical models. However, we will show here that even this explanation is not viable: the high-redshift progenitors of the dSph appear to have been fundamentally different from the building blocks of the Milky Way.

In this Letter, we study the metallicity distribution of a large sample of stars in four nearby dSph: Sculptor, Fornax, Sextans and Carina. The data presented here were taken using the European Southern Observatory (ESO) VLT/FLAMES facility in low-resolution (LR) mode (Pasquini et al. 2002). The DART programme has observed Sculptor, Fornax and Sextans, while the data for Carina comes from the ESO archive.

### 2. OBSERVATIONS AND ANALYSIS

For each galaxy we derive metallicity estimates as well as accurate radial velocity measurements for several hundred red giant branch (RGB) stars located over a large area extending out to the tidal radius (Tolstoy et al. 2004, Koch et al. 2006, Battaglia et al. 2006). We use RGB stars for our spectroscopic program, since they are bright, cover a range of ages dating back to the oldest stellar populations in these galaxies (Stetson, Hesser & Smecker-Hane 1998), and (the majority) are believed to contain in their atmospheres an unpolluted sample of the metallicity of the interstellar medium out of which they formed. To identify candidate RGB stars in the dSph we used ESO Wide Field Imager observations to construct colour-magnitude diagrams and selected giant branch stars from their well-defined locii. We took particular care to acquire a statistically fair sample by targeting potential RGB members over a wide range in colour and in spatial location, in order to probe the more evenly distributed metal-poor component (although we only have a small number of stars lo-

<sup>1</sup> Based on FLAMES/GIRAFFE observations collected at the European Southern Observatory, proposal 171.B-0588

<sup>2</sup> Kapteyn Astronomical Institute, University of Groningen, P.O.Box 800, 9700 AV Groningen, The Netherlands; ahelmi@astro.rug.nl

<sup>3</sup> Institute of Astronomy, University of Cambridge, Madingley Road, Cambridge CB3 0HA, UK

<sup>4</sup> Observatoire de Paris, section de Meudon, 5 Place Jules Janssen, F-92195 Meudon Cedex, France

<sup>5</sup> Laboratoire d'Astrophysique, Ecole Polytechnique Fédérale de Lausanne (EPFL), Observatoire, CH-1290 Sauvigny, Switzerland. On leave from CNRS-UMR8111, Observatoire de Paris

<sup>6</sup> Department of Physics and Astronomy, University of Victoria, 3800 Finnerty Road, Victoria, BC, V8P 1A1, Canada

<sup>7</sup> University of Texas, McDonald Observatory, Fort Davis, Texas, USA

<sup>8</sup> National Astronomical Observatory of Japan, 2-21-1 Osawa, Mitaka, Tokyo 181-8588, Japan

<sup>9</sup> Kavli Institute for Particle Astrophysics and Cosmology, 2575 Sand Hill Road, Menlo Park, CA 94044, USA

<sup>10</sup> European Southern Observatory, Alonso de Cordova 3107, Santiago, Chile

<sup>11</sup> European Southern Observatory, Karl-Schwarzschildstr. 2, D-85748 Garching bei München, Germany

<sup>12</sup> Astronomical Institute, Osaka Kyoiku University, Asahigaoka, Kashiwara, Osaka 582-8582, Japan

cated near the tidal radius). For example, in Sextans we have obtained spectra for every RGB star candidate over several square degrees down to  $V=20$  ( $M_V=0.6$ ), while for Sculptor more than 50% of the brighter RGB stars out to the notional tidal radius have been followed up.

We use the CaII triplet region of the RGB star’s spectrum to estimate its metallicity (Cole et al. 2004). This indicator requires only low or intermediate spectral resolution, is based on three absorption lines around  $8500\text{\AA}$ , and has been empirically calibrated from high-resolution abundance studies of stars in globular clusters (Armandroff & Da Costa, 1991).

All spectroscopic VLT/FLAMES observations were made in Medusa mode, in which  $\sim 120$  fibres are placed over a 25 arcmin diameter field of view. The data were all reduced, extracted and wavelength calibrated using the pipeline provided by the FLAMES consortium (Blecha et al. 2003). For sky subtraction, velocity and equivalent width estimation, we developed our own software which was thoroughly checked on multiple observations of the same fields taken at different times. From the equivalent width of the individual CaII triplet lines  $EW$ , we estimate the metallicity as (Tolstoy et al. 2001):

$$[\text{Fe}/\text{H}] = -2.66 + 0.42 [EW_{2+3} + 0.64 (V - V_{HB})] \quad (1)$$

where  $EW_{2+3}$  is the combined equivalent width derived from lines 2 and 3, and  $V - V_{HB}$  is the apparent magnitude difference between the star and the horizontal-branch of the system (i.e. a proxy correction for the effect of surface gravity). We find that for reliable  $[\text{Fe}/\text{H}]$  determinations ( $\pm 0.1$  dex) a continuum signal-to-noise  $S/N \geq 10$  per  $\text{\AA}$  is required. In what follows, we consider only those stars satisfying this criterion and also with estimated radial velocity errors less than 6 km/s.

The velocities, metallicities and spatial distribution of the stars in our survey are shown in Fig. 1. We identify velocity members of a particular dwarf galaxy by applying a  $\sigma$ -clipping procedure, and retaining those stars within  $3\text{-}\sigma$  of the converged mean velocity (typically  $\pm 35$  km/s). There are 364 member stars in our Carina sample, 933 in Fornax, 513 in Sculptor and 202 in Sextans.

### 2.1. The low-metallicity tail

The metallicity distributions of the galaxies are shown in Fig. 2. There is great diversity from system to system, which reflects their widely different star formation and chemical enrichment histories (e.g. Mateo 1998). There is, however, a common denominator: contrary to naive expectations, there is a dearth of stars with  $[\text{Fe}/\text{H}] < -3$  dex.

We have carried out a number of checks to confirm the reality of this result, and to rule out systematic errors that would prevent us from finding  $[\text{Fe}/\text{H}] < -3$  dex from our LR CaII spectra. Firstly, we have compared our FLAMES LR CaII measures with FLAMES high-resolution measures based directly on FeI and FeII lines and find good agreement (i.e. within 0.1 to 0.2 dex), over the range  $-2.5 < [\text{Fe}/\text{H}] < -0.5$  for the Sculptor and Fornax samples (Battaglia et al., in prep). Secondly, we have followed up with high resolution spectroscopy, several of the metal-poor objects with  $[\text{Fe}/\text{H}] \sim -2.7$  and find similarly good agreement with our LR metallicity estimates. Finally, we have carried out an extensive search for continuum-only CaII objects in our samples, and found very few candidates. These have turned out to be nearby subdwarfs or distant galaxies in follow-up high-resolution spectra with larger wavelength coverage (Venn et al., in prep).

We now focus on the low-metallicity tail of the distributions ( $[\text{Fe}/\text{H}] \lesssim -2.4$  dex). The panels on the right of Fig. 2 show

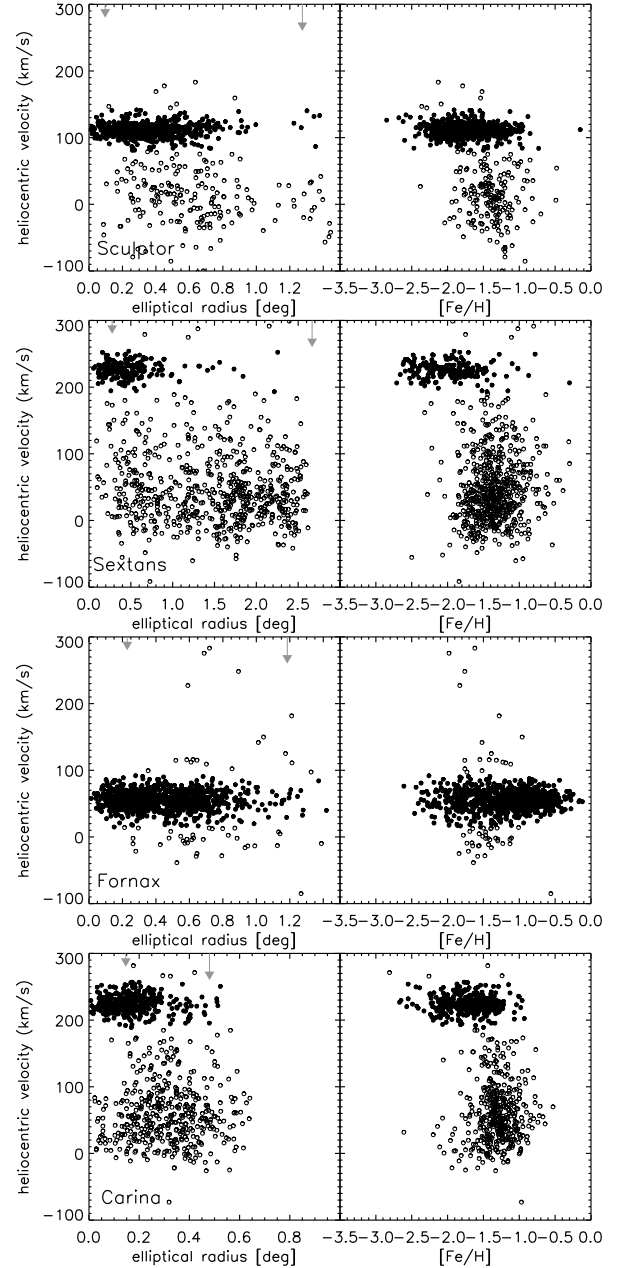


FIG. 1.— Velocities of stars in four dSph (solid symbols), as function of elliptical radius (left) and metallicity (right). The arrows on the left panels denote the core and tidal radius of the galaxies. Note that the foreground dwarf (open symbols) metallicities are token values; nevertheless the velocity vs.  $[\text{Fe}/\text{H}]$  diagrams are generally a useful diagnostic of membership.

the (unbinned) cumulative distribution of metallicities for the dSph. This distribution is less sensitive to small numbers statistics than the differential one shown in the left-handside panels. The exponential shape of the low-metallicity tail can be explained in the context of a closed-box model of chemical evolution with initial enrichment (e.g. Pagel 1998). In this model the number of stars with abundances lower than  $Z$  is

$$N(< Z) = A(1 - \exp\{- (Z - Z_0)/p\}) \quad (2)$$

where  $A$  depends on the initial gas mass available for star formation,  $Z_0$  is the initial abundance of the gas, and  $p$  is the yield. In the regime considered here,  $Z/Z_\odot \sim (10^{-4} - 10^{-2.5})$ , and so we can linearize Eq.(2) to obtain  $N(< Z) \sim$

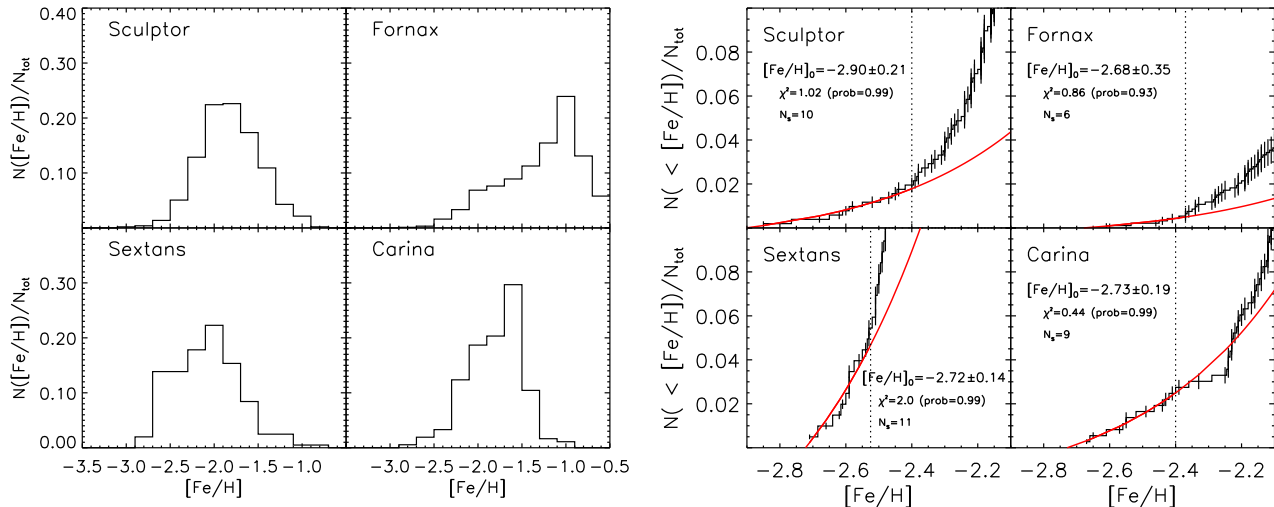


FIG. 2.— *Left*: Differential metallicity distribution of the dSph. *Right*: Cumulative metallicity distributions (error bars are Poissonian). The solid curve corresponds to the least squares model fit to the low metallicity tail (defined by the  $N_S$  stars located to the left of the vertical dotted line).

$A(Z - Z_0)/p$ . If we express  $Z = Z_\odot 10^{[\text{Fe}/\text{H}]}$ , then

$$N(<[\text{Fe}/\text{H}]) = a \exp([\text{Fe}/\text{H}] \ln 10) + b \quad (3)$$

where  $a = AZ_\odot/p$ , and  $b = -a \exp([\text{Fe}/\text{H}]_0 \ln 10)$ . Therefore the ratio  $b/a$  directly depends on the initial metallicity  $[\text{Fe}/\text{H}]_0$  of the gas from which the stars formed. The grey curves shown in the panel on the right of Fig. 2 correspond to the model fits to the low-metallicity tail of the distribution. In all cases, we find very good fits to the data, and are able to obtain a reliable estimate of  $[\text{Fe}/\text{H}]_0$ .

This analysis shows that the interstellar medium (gas) in each of these dwarf galaxies had been enriched to  $[\text{Fe}/\text{H}] \sim -3$  dex prior to the earliest star formation episode that led to the present-day stellar population. It is intriguing that this lowest metallicity is very similar for all four galaxies, despite their widely different characteristics. This suggests that the gas had been enriched very uniformly over a (co-moving) volume of  $\sim 1 \text{ Mpc}^3$  (i.e. that occupied by the Local Group) very early-on. This conjecture would also seem to be supported by the metallicity distribution of Galactic halo globular clusters which does not extend below  $-2.4$  dex (e.g. Harris 1996).

## 2.2. Comparison to the Galactic halo

To establish the relation between the dwarf satellites of our Galaxy and its putative building blocks, we now compare the metal-poor tail of the metallicity distributions of the dSph and the Galactic halo. By focusing on the low-metallicity tail we aim to test whether the first generations of stars in the dwarfs were analogous to those in the Galactic building blocks.

The halo metallicity distribution function has been intensively studied for more than three decades because of its power to constrain Galaxy evolution models. Ryan & Norris (1991) were the first to show that the metal-poor tail extends well below  $[\text{Fe}/\text{H}] \sim -3$  dex, on the basis of a sample of 240 kinematically-selected halo stars, in which only 5 stars were found to have such low metallicities. Although this is a small number of objects, this sample size was already smaller than what is typical for the dSph in the DART program.

More recently, the HK and the Hamburg/ESO (HES) surveys have yielded a dramatic increase in the number of metal-poor stars known (Beers & Christlieb 2005). In these surveys, metal-poor candidates are selected from objective-prism spectra for which the Ca H and K lines are weaker than expected at

a given  $(B - V)$  colour. These stars are then followed up with medium resolution spectroscopy<sup>13</sup>. By construction, a bias is introduced at metallicities  $[\text{Fe}/\text{H}] > -2.5$  dex, implying that the shape is only well-constrained below this value.

The HES survey contains  $\sim 40$  giants with  $[\text{Fe}/\text{H}] < -3.0$  dex; 130 stars with  $[\text{Fe}/\text{H}] < -2.5$  dex and  $\sim 400$  stars with  $[\text{Fe}/\text{H}] < -2.0$  dex (Christlieb, Reimers & Wisotzki 2004). We have 320 stars in the dSph with  $[\text{Fe}/\text{H}] < -2.0$  dex, of which only 29 have  $[\text{Fe}/\text{H}] < -2.5$  dex, and none have  $[\text{Fe}/\text{H}] < -3.0$  dex. The contrast is stark, but could our inability to find very metal-poor stars ( $< -3$  dex) in the dSph be an artifact of the sample size?

We have quantified the significance of this issue by adopting the conservative approach of only considering stars with  $[\text{Fe}/\text{H}] < -2.5$  dex, where the HES survey is most likely to be complete. We bootstrapped the HES metallicity distribution below  $[\text{Fe}/\text{H}] \sim -2.5$  dex to make random subsets of 10 stars, which is the typical number we have below  $-2.5$  dex for any one of our dSph samples. We then derive the mean distribution for 1000 such subsets. This is the solid histogram shown in Fig. 3. While it is clear that we are in the small numbers statistics regime, Fig. 3 unambiguously shows that even this bootstrapped distribution is significantly different from that of the dSph. By means of a Kolmogorov-Smirnov test, we have quantified the probability that the bootstrapped HES distribution is consistent with the metallicity distribution of each individual dwarf galaxy. We find that the probability is very low in all cases, ranging from  $8 \times 10^{-4}$  for Sextans, to  $4 \times 10^{-3}$  for Carina and  $8 \times 10^{-3}$  for Sculptor and Fornax.

## 3. DISCUSSION

The above analyses show that the tails of the metallicity distributions of the dSph and the Galactic halo are very different at highly significant levels. Contrastingly, the metallicity distributions at low  $[\text{Fe}/\text{H}]$  of all dSph are consistent with one another at the  $1-\sigma$  level; the observed lack of very metal-poor stars might be considered to be a kind of ‘‘G-dwarf problem’’ on the scale of the dwarf spheroidal galaxies.

<sup>13</sup> Barklem et al. (2006) have carried out a high-resolution study of a large subset of stars from the HES survey, and found good agreement with the Ca HK metallicity estimates.

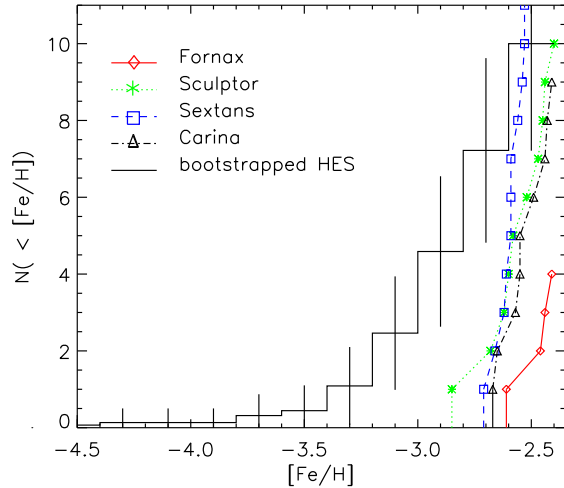


FIG. 3.— Comparison of the cumulative metallicity distributions of the stars in the mean bootstrapped HES sample and in the dSph.

This implies that any merging, even very early merging, of the progenitors of the nearby dwarf galaxies as a mechanism for building up the Galactic halo is ruled out. The absence of very metal-poor stars in the dSph shows that the progenitors of the Milky Way and the dSph must have been different.

We can think of two possible explanations. In the first scenario the Galactic building blocks formed from the collapse of high- $\sigma$  density fluctuations in the early Universe (Diemand et al. 2005), while the dwarf satellites would stem from low- $\sigma$  peaks, predicted to collapse on average at much lower redshifts; e.g., a 1- $\sigma$  density fluctuation of mass  $10^8 M_\odot$  collapses at  $z \sim 4$  in a  $\Lambda$ CDM universe (e.g. Qian & Wasserburg 2004). It is interesting to note that absorption line spectra towards quasars show that the intergalactic medium at this redshift has a mean metallicity of  $[\text{Fe}/\text{H}] \sim -3$  dex (Cowie & Songaila 1998), a value that is consistent with the lowest metallicity

stars found in our sample. This would mean the oldest stars in the dSph are  $\sim 12$  Gyr old, formed after the Universe was reionized and from a pre-enriched intergalactic medium.

A second explanation could be that the initial mass function (IMF) behaved differently in Galactic building blocks and dSph at the earliest times. This is a possible interpretation of the observational fact that the Galactic halo contains some very metal poor stars with mass  $\sim 0.8 M_\odot$  (Christlieb et al. 2002; Frebel et al. 2005) which are not seen in dSph. For example, in the case of a bimodal IMF, low-mass stars can form even from zero metallicity gas (Nakamura & Umemura 2001). However, this is only possible if the initial density of the gas is sufficiently large, and so this would be favoured in high- $\sigma$  peaks collapsing at very early times.

It may be possible to distinguish between the two scenarios proposed above through detailed chemical abundance studies. Unfortunately, the currently available high resolution spectra of metal-poor stars in dSph is very sparse with only a few published examples of stars below  $-2.5$  dex (e.g. Shetrone et al. 2001; Sadakane et al. 2004; Fulbright, Rich & Castro 2004) and as such is still inconclusive.

In both scenarios, the key element is the bias in the galaxy formation process, while environment would seem to play a less important role. However, clearly the models need to be explored in much more detail than the mere outline given here. These efforts should be supplemented by large observational programs, which should not just focus directly on the high-redshift distant universe. There is much to learn about what happened at those early epochs from our own backyard.

This work was partially supported by the Netherlands Organization for Scientific Research (AH), the Royal Netherlands Academy of Arts and Sciences (ET), and the U.S. National Science Foundation (AST-0306884, MDS; AST-0239709, TA). We would like to thank the Aspen Center for Physics for its hospitality.

#### REFERENCES

- Armandroff, T.E. & Da Costa, G.S. 1991, *AJ*, 101, 1329  
 Barklem, P.S., et al. 2005, *A&A*, 439, 129  
 Battaglia, G. et al. 2006, *A&A* (in press; astro-ph/0608370)  
 Beers, T.C. & Christlieb, N. 2005, *ARA&A*, 43, 531  
 Blecha, A., North, P., Royer, F. & Simond, G. 2003 *BLDR Software Reference Manual 1.09*, Doc. No. VLT-SPE-OGL-13730-0040  
 Bromm, V. & Larson, R.B. 2004, *ARA&A*, 42, 79  
 Christlieb, N. et al. 2002, *Nature*, 419, 904  
 Christlieb, N., Reimers, D. & Wisotzki, L. 2004, *The Messenger*, 117, 40  
 Cole, A.A., Smecker-Hane, T.A., Tolstoy, E., Bosler, T.L. & Gallagher, J.S. 2004, *MNRAS*, 347, 367  
 Cowie, L.L. & Songaila, A. 1998, *Nature*, 394, 44  
 Diemand, J., Madau, P., & Moore, B. 2005, *MNRAS*, 364, 367  
 Font, A. S., Johnston, K. V., Bullock, J. S., & Robertson, B. E. 2006, *ApJ*, 638, 585  
 Frebel A., et al. 2005, *Nature*, 434, 871  
 Fulbright, J. P., Rich, R. M., & Castro, S. 2004, *ApJ*, 612, 447  
 Gnedin, N. Y., & Kravtsov, A. V. 2006, *ApJ*, 645, 1054  
 Grebel, E.K. & Gallagher, J.S. 2004, *ApJ*, 610, 89  
 Harris, W.E. 1996, *AJ*, 112, 1487  
 Koch, A., et al. 2006, *AJ*, 131, 895  
 Mateo, M.L. 1998, *ARA&A*, 36, 435  
 Nakamura, F. & Umemura, M. 2001, *ApJ*, 548, 19  
 Pagel, B.E.J. 1998, *Nucleosynthesis and chemical evolution of galaxies*. Cambridge Univ. Press  
 Pasquini, L., et al. 2002 *ESO Messenger* 110, 1  
 Pritzl, B. J., Venn, K. A., & Irwin, M. 2005, *AJ*, 130, 2140  
 Qian, Y.-Z. & Wasserburg, G.J. 2004, *ApJ*, 612, 615  
 Ryan, S.G. & Norris, J.E. 1991, *AJ*, 101, 1865  
 Sadakane, K., Arimoto, N., Ikuta, C., Aoki, W., Jablonka, P. & Tajitsu, A. 2004, *PASJ*, 56, 1041  
 Shetrone, M. D., Côté, P., & Sargent, W. L. W. 2001, *ApJ*, 548, 592  
 Stetson, P. B., Hesser, J. E., & Smecker-Hane, T. A. 1998, *PASP*, 110, 533  
 Tolstoy, E. et al. 2001, *MNRAS*, 327, 918  
 Tolstoy, E. et al. 2004, *ApJ*, 617, 119  
 Unavane M., Wyse, R. F. G., & Gilmore, G. 1996, *MNRAS*, 278, 727  
 Venn, K.A., et al. 2004, *AJ*, 128, 1177